Article

A Digital Twinning Approach for the Internet of Unmanned Electric Vehicles (IoUEVs) in the Metaverse

Mohsen Ebadpour [1,*] , Mohammad (Behdad) Jamshidi [2] , Jakub Talla [1], Hamed Hashemi-Dezaki [1,*] and Zdeněk Peroutka [1]

1   Research and Innovation Center for Electrical Engineering (RICE), Faculty of Electrical Engineering, University of West Bohemia (UWB), 30100 Pilsen, Czech Republic
2   Faculty of Electrical Engineering, University of West Bohemia (UWB), 30100 Pilsen, Czech Republic
*   Correspondence: ebadp@fel.zcu.cz (M.E.); hhashemi@fel.zcu.cz (H.H.-D.)

Abstract: Regarding the importance of the Internet of Things (IoT) and the Metaverse as two practical emerging technologies to enhance the digitalization of public transportation systems, this article introduces an approach for the improvement of IoT and unmanned electric vehicles in the Metaverse, called the Internet of Unmanned Electric Vehicles (IoUEVs). This research includes two important contributions. The first contribution is the description of a framework for how unmanned electric vehicles can be used in the Metaverse, and the second contribution is the creation of a digital twin for an unmanned electric vehicle. In the digital twin section, which is the focus of this research, we present a digital twin of an electronic differential system (EDS) in which the stability has been improved. Robust fuzzy logic algorithm-based speed controllers are employed in the EDS to independently control the EV wheels driven by high-performance brushless DC (BLDC) electric motors. In this study, the rotor position information of the motors, which is estimated from the low-precision Hall-effect sensors mounted on the motors' shafts, is combined and converted to a set of common switching signals for empowering the EDS of the electric vehicle traction drive system. The proposed digital twin EDS relies on an accurate Hall sensor signals-based synchronizing/locking strategy with a dynamic steering pattern capable of running in severe road conditions with different surface profiles to ensure the EV's stability. Unlike recent EDSs, the proposed digital twinning approach includes a simple practical topology with no need for auxiliary infrastructures, which is able to reduce mechanical losses and stresses and can be adapted to IoUEVs more effectively.

Keywords: electronic differential system; electric vehicle (EV); digital twin; brushless DC (BLDC) motors; stability control; Internet of Unmanned Electric Vehicles (IoUEVs); Metaverse

1. Introduction

The energy crisis has led to an increase in the shortage of fossil fuel resources that are mostly responsible for environmental pollution issues, contributing to the development of hybrid or pure electric vehicles. Pure electric vehicles (EVs), which are also called battery EVs (BEVs), have reduced the dependence on fossil fuels by using green electric energy instead of fossil fuel resources, which is more effective than in conventional cars with internal combustion engines [1]. Various electric propulsion systems along with specific driving cycles have been presented for both manned and unmanned EVs based on their types of steering and differential systems [2–5]. To decrease the weight and size of an EV traction drive system, an electronic differential system (EDS) with an effective control strategy is utilized instead of conventional mechanical transmission and steering systems [6,7]. A suitable EDS in EVs can elevate the vehicle's stability during uncertain road surface conditions, equally distribute mechanical force impacts to the wheels, diminish mechanical losses, and take advantage of electric motors in all-wheel drive systems [8]. In addition, the safety of passengers in EVs can be increased during slippery and sloping

roads using the EDS by separately controlling the traction wheels' velocity and active torque distribution.

There are several types of electronic differentials based on the limited-slip differential method or the torque vectoring differential approach for EVs equipped with two-wheel drive (2WD) and four-wheel drive (4WD) propulsion systems. The locking of the wheels' differential system based on sync-lock controlled independent brushless DC (BLDC) traction motor drives was studied in [9]. The locking algorithm is modeled using the position signals of the BLDC motors and operating them with a set of averaged signals at the identical speed and rotor angle. However, this approach suffers from stability during large angle differences between the motor shaft position and sudden variations of the wheels' torque. The authors in [10] conducted research on Ackermann's geometric differential model for EDS using a dual-rotor permanent magnet synchronous motor using a coordination control strategy for EV applications. The simulation results illustrated better performance for the vehicle during different transient and steady-state operations; however, the traction drive system requires an auxiliary circuit in the power supply part.

Three-phase synchronous BLDC motors are mostly employed in electric car industries and aerospace due to their merits of high stability, low inertia, high power density, low loss, and simple control [11–13]. In [14], a 2WD system equipped with rear shaft EDS empowered by BLDC motors is used to independently drive an EV's wheels using fuzzy logic controllers. An embedded digital EDS on two BLDC motor drives for the steering control of an EV is investigated in [15] to balance the rotational speed between two traction motors and improve the efficiency of the vehicle's performance. The embedded EDS with digital implementation makes the EV propulsion system more efficient due to better tracking of the reference speed of the motors; however, it reduces the overall stability of the EV during sharp steering angle variations. The optimization of EDS topology with a modified speed control algorithm is studied in [16] for EVs using the full model of in-wheel BLDC motors. The controller coefficients are properly tuned to reduce the traction motors' power usage by considering two constraints with the lowest torque saturation and wheel slippages. The independent control of the rear shaft's steering angle driven by the BLDC motors for a 2WD EV based on a fuzzy logic speed controller in a GUI interface is established in [17] using auxiliary current regulators to generate signals for the inverter switching devices. From the literature review, it can be concluded that the main target of a suitable EDS is ensuring EV stability during unequal road surface conditions as well as improving passengers' safety in bumpy driving cycles. However, most of the previous EDS topologies use conventional velocity controllers with weak stability and, in most cases, include auxiliary elements, leading to an increase in the cost and complexity of the drive system.

In the last two decades, the high competition in the EV market due to increasing demand has led to emerging of many companies to develop their green vehicles in a vast range of scopes. To sustainably improve the problem of environmental emissions, intelligent but feasible solutions are in more demand, one of the effective solutions being the employing digital twin (DT) technology [18]. The concept of a DT refers to a twin of an actual process or physical asset in a simulation or a digital platform. They are implemented from physical twins ranging from giant objects such as airplane actuators and vehicles to tiny devices such as integrated circuits and micro-switches [19]. By integrating the features of the Internet of Things (IoT) and the most recent software featuring machine learning, the efficiency of DT can be successfully improved. With simulation tools, researchers can implement an enormous number of implementations on any DT, which is difficult on a physical asset. The DT performs as a desired platform along with IoT architectures to map the offline physical device to a DT model [20]. With the large amount of sensory information that an EV's drive system produces, DT technology is considerably more appealing than other tools such as hardware-in-the-loop evaluations. This process enables intelligent system monitoring, fault diagnosis, and the estimation of states, and improves the useful lifetime period [21].

In this article, a digital model of an EV empowered by an optimized EDS is proposed, equipped with independent BLDC traction motors controlled by robust fuzzy logic speed commanders. The proposed digital twinning EDS operates using a group of averaged virtual Hall signals to precisely drive the EV at all driving cycles without degrading the vehicle stability. To ensure car safety, the speeds and torques of the electric motors are separately controlled through a variable DC-link voltage of the propulsion inverter with no auxiliary current or voltage regulators. By employing DT and IoT features, an efficient drive system is built that optimizes the BLDC motors' performance and EV power trains. The position information of the motors' shafts, derived from the Hall-effect sensors, is used as inputs to a DT model to develop models for the EDS of the EV. The proposed EDS improves the overall stability of the vehicle at an acceptable rate during severe road conditions by properly controlling the steering angle in curved cycles. The organization of this article is as follows. In Section 2, the DT technology and the IoT of EVs are explained. In Section 3, the DT of the overall traction drive system of the EV is analyzed, including the dynamic model of the vehicle and the mathematical model of the BLDC motors. Section 4 describes the EDS topology and control system, relying on the robust smart fuzzy algorithm. In Section 5, the simulation results are illustrated. Finally, a discussion of the overall methodology and system performance is summarized and the conclusion is presented in Section 6.

2. Digital Twin of Internet of Unmanned Electric Vehicle (IoUEV) in Metaverse

From a transportation perspective, the "virtual world" is a digital version of actual transportation systems such as roads, cars, and weather. This digital version is also referred to as the "Metaverse" and is utilized for testing and improving various transportation scenarios, which can result in a better real-life transportation system [22–25]. The virtual world of transportation includes fixed objects such as buildings, moving objects such as cars, weather patterns such as rain or snow, seasonal variations such as blooming flowers, and light sources such as streetlights and headlights. It is crucial for stationary objects to look like their real-life counterparts, and for moving objects to have features that work similarly to real-life objects. For instance, cars in the virtual world must accelerate, brake, and steer as they do in the real world. Moreover, the virtual world must follow the laws of physics, such as daylight and nighttime conditions and the corresponding light sources. The accuracy of the virtual world is essential in minimizing the gap between the virtual and real worlds. This, in turn, enables transportation professionals to test and optimize various transportation scenarios more efficiently, leading to better real-life transportation systems. In other words, the virtual realm of transportation encompasses numerous components such as fixed objects, moving objects, weather patterns, seasonal variations, and sources of light. In virtual space, the visual attributes of stationary objects are akin to their physical counterparts, while active objects must possess functional features that resemble real-life counterparts. Additionally, weather and seasonal changes directly impact the visual rendering, which must conform to physical laws. For example, springtime brings forth blossoming plants, daylight hours are accompanied by sunlight, and nighttime is illuminated by streetlights and vehicle headlights. Maintaining the accuracy of the virtual space can significantly reduce the disparity between the two coexisting spaces.

The suggested framework for IoUEVs in the Metaverse comprises five layers, as shown in Figure 1, with each layer fulfilling a distinct objective and aiding in enhancing the caliber of the IoUEV and its applications in the Metaverse. The following paragraphs provide a detailed account of every layer.

Metaverse as layer 1: The first layer of the proposed model holds paramount importance as it forms the basis on which the subsequent layers are constructed. The Metaverse, a digital realm designed for social interaction and the manipulation of virtual objects, serves as a platform for managing IoUEV transportation in this model. The integration of diverse technologies and systems, such as IoUEVs, Intelligent Transportation Systems (ITS) networks, and navigation systems, within the Metaverse enables the creation of a seamless and efficient transportation system. The cooperative interaction of these technologies ensures a

dependable, secure, and sustainable transportation experience within the Metaverse. Layer 2 of the proposed model is called the Intelligent Transportation Systems (ITS) network. This layer consists of many connected systems and technologies that help manage IoUEV transportation. The ITS network is made up of different parts, such as traffic management systems, communication systems, and vehicle tracking systems. These components work together to make sure that IoUEVs move around the Metaverse safely and efficiently.
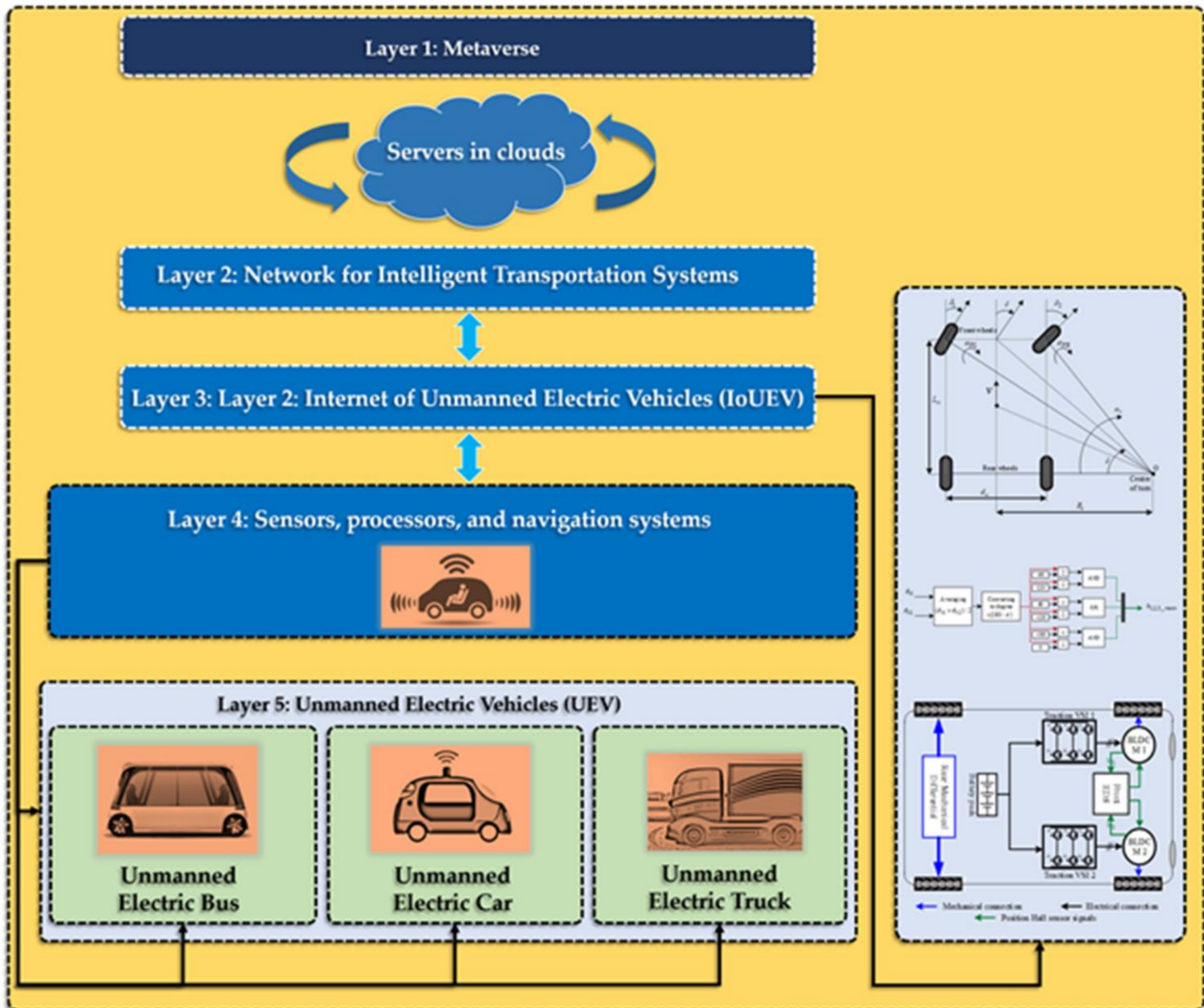

Figure 1. The proposed model for the Internet of Unmanned Electric Vehicles (IoUEVs) in the Metaverse comprises five layers that aim to improve the quality of the IoUEV and its applications within the Metaverse. These layers are designed with specific purposes and include the Metaverse as layer 1, an Intelligent Transportation Systems network as layer 2, IoUEV as layer 3, sensors, processors, and navigation systems as layer 4, and unmanned electric vehicles as layer 5. The framework utilizes cutting-edge technologies, such as the Metaverse, IoUEVs, and autonomous vehicles, to create a smooth and efficient transportation experience. By optimizing each layer, the transportation system is managed comprehensively.

The third layer of the proposed model is the IoUEV. This layer includes unmanned electric vehicles that can operate independently in the Metaverse. These vehicles are equipped with advanced sensors, processors, and navigation systems that enable them to navigate through complex virtual environments on their own. IoUEVs are also powered by electricity, which makes them environmentally friendly and cost effective. The fourth layer of the proposed model involves sensors, processors, and navigation systems. These technologies

allow IoUEVs to function independently in the Metaverse. The layer encompasses a range of sensors, such as radars, cameras, and LiDAR, which provide real-time information about the vehicle's surroundings [26–30]. Processors, including microcontrollers and microprocessors, are responsible for processing this information and enabling the IoUEVs to make decisions about their movements. Navigation systems, such as GPS and inertial measurement units (IMUs), provide accurate location and orientation data to IoUEVs. Layer 5 of the proposed model is Unmanned Electric Vehicles. This layer consists of the physical IoUEVs that function within the Metaverse. The vehicles are environmentally friendly, energy efficient, and prioritize safety. Additionally, they are equipped with advanced technologies such as sensors and navigation systems, allowing them to operate independently.

3. Digital Twin of the EV System

As mentioned previously, digital twins play an effective role in the development of the EV industry, which, when debated among consumers, improves products' quality with high reliability in their performance. However, the concept of DT technology goes decently beyond just the optimization of the production and the operations of EVs. It implies to the consumer a desired approach in which EVs are different in comparison with the conventional vehicles in terms of the propulsion system and overall topology, which has been a key factor in altering EVs for safe transportation cars. Regarding this study, an accurate mathematical model to perform digital twins of the EV traction drive system contains the BLDC motors' model, vehicle dynamic model, and EDS implementation model in more detail. In this section, the DT model of the EV system, which is based on the dynamic behavior of the BLDC motor drives, is explained. Here, the main goal is to practically model the traction drive system of the EV to provide digital twins for model-based applications.

3.1. Traction Motor Drive Model

To successfully enter EVs into the automobile market, several design and control requirements should be taken into account. The first concern is the traction drive design of the vehicle in an appropriate computer-aided software platform. Accordingly, EV researchers begin to model and then design the vehicle's aerodynamic infrastructures along with its traction electric motors. Digital prototyping has also made headway recently with the arrival of DT technology that allows car producers to assemble physical electric motors of their designs quickly for performance monitoring and vital variable predictions [31]. Three-phase BLDC motors are especially well designed for EV applications due to equipping to high-power permanent magnets, which allow vast acceleration rates, combined with high-performance drives and speed ranges of up to 12,000 rpm. The rotor position signal is fed electronically through three low-precise, cost-effective Hall-effect sensors offset by 120° [32]. These motors require a three-phase voltage source inverter (VSI) to run. Here, the switching pulses of the VSI switching devices are determined by utilizing the Hall sensor signals to detect the rotor position [9]. In this study, two identical BLDC motors are deployed as traction drives for the 2WD electric vehicle that is going to be implemented.

Figure 2 illustrates the electric circuit of a three-phase BLDC motor drive. These motors are generally controlled by employing a three-phase VSI, a rotor position sensor for providing an appropriate commutation signal to fire the inverter's switching devices. The rotor position sensor can be a set of low-precise Hall sensors or high-precise shaft encoders. As can be seen in Figure 3, the switching interval for each stator's phase is 120 electrical degrees. Only two phases conduct current at any interval, leaving the third phase floating. To produce the maximum torque density, the inverter should be commutated every 60° so that the current is in phase with the back-EMF.
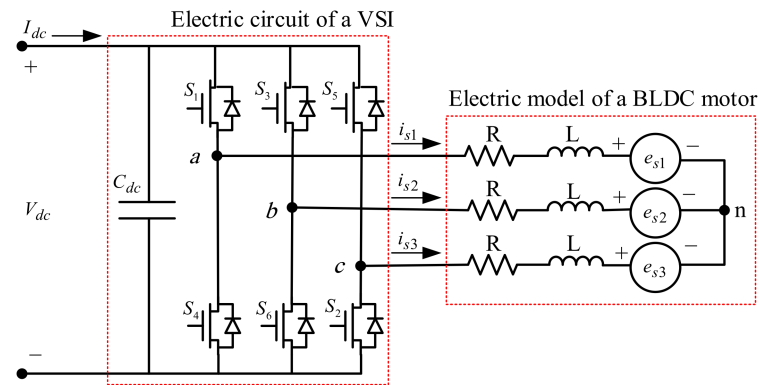
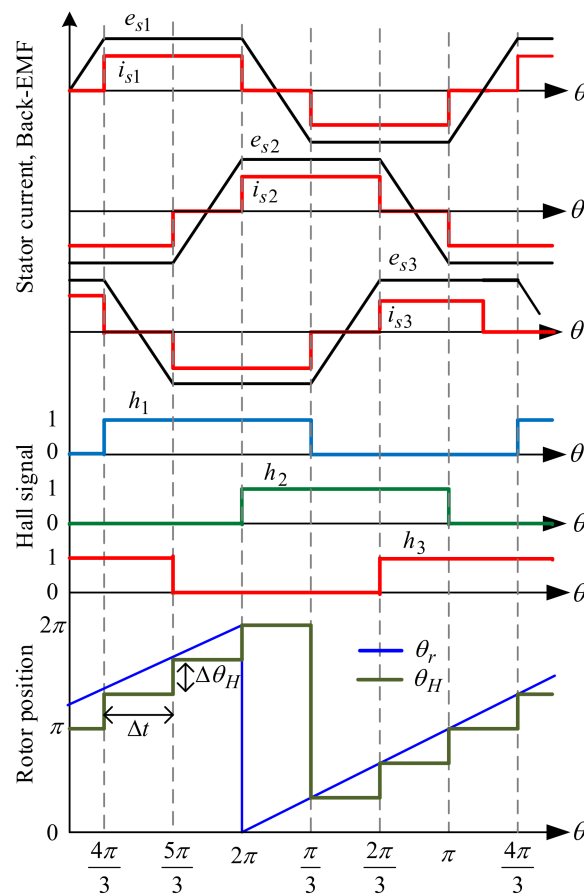**Figure 2.** Electric circuit of a three-phase BLDC motor drive.

Figure 3. Electrical waveforms and mechanical signals of a BLDC motor under normal operation.

According to Figure 3 (bottom subplot), the time durations of each switching interval s Δt along with the quantized position θ_H by the Hall signals are utilized to estimate the high-precise rotor position θ_r and motor speed. The rotor speed can be obtained by calculating the changes in quantized position deference $\Delta\theta_H$ over the corresponding time intervals, as

$$\omega_r(t) = \frac{\Delta\theta_H}{\Delta t} = \frac{\pi/3}{\Delta t}. \tag{1}$$

The high-precise rotor position θ_r can then be approximated by combining the rotor speed in (1) within each interval as

$$\theta_r(t) = \theta_H + \int_0^{\Delta t} \omega_r(t)dt. \tag{2}$$

In order to model and simulate the BLDC motor drive, the rotor position θ_r, the stator currents $i_{s1,s2,s3}$, and the voltages $v_{s1,s2,s3}$ are required. The electric function for a k-phase BLDC motor is expressed as [33]

$$v_{sk} = R \cdot i_{sk} + L \cdot \frac{di_{sk}}{dt} + e_{sk}, \tag{3}$$

where L and R are the inductance and resistance of each stator phase for phase numbers $k = 1, 2, 3$, respectively. From the trapezoidal shape of back-EMFs in the BLDC motor e_{sk}, the electromagnetic torque T_{em} of the motor shaft can be calculated as

$$T_{em} = \frac{1}{\omega_m} \sum_{k=1}^{3} (e_{sk} \cdot i_{sk}) = P \cdot \lambda_M \sum_{k=1}^{3} F\left(\theta - (k-1)\frac{2\pi}{3}\right) \cdot i_{sk}, \tag{4}$$

in which P is the number of pole pairs and λ_M is the maximum flux of rotor permanent magnets (PMs). $F(\theta)$ shapes the rotor angle in trapezoidal form.

3.2. Vehicle Dynamics Model

Evaluating electric vehicle dynamics might be an arduous target in multi-objective modeling. Vehicle aerodynamic systems are more complicated with every new generation of EV topologies, and each EV includes an effect on the other topologies. The EV's power-train system needs to interact with other components and consider the vehicle-level impact of the features they are including. Several dynamic configurations have been implemented for EVs with 2WD, 4WD, and all-wheel drive (AWD) propulsion systems. In this article, the front 2WD EV topology with a separate speed control of the BLDC motor drives is studied by employing a pair of three-phase VSI circuits. Considering Figure 4, the topology of the EV shows the motors that run the front wheels, while the rear ones contain a mechanical differential system.
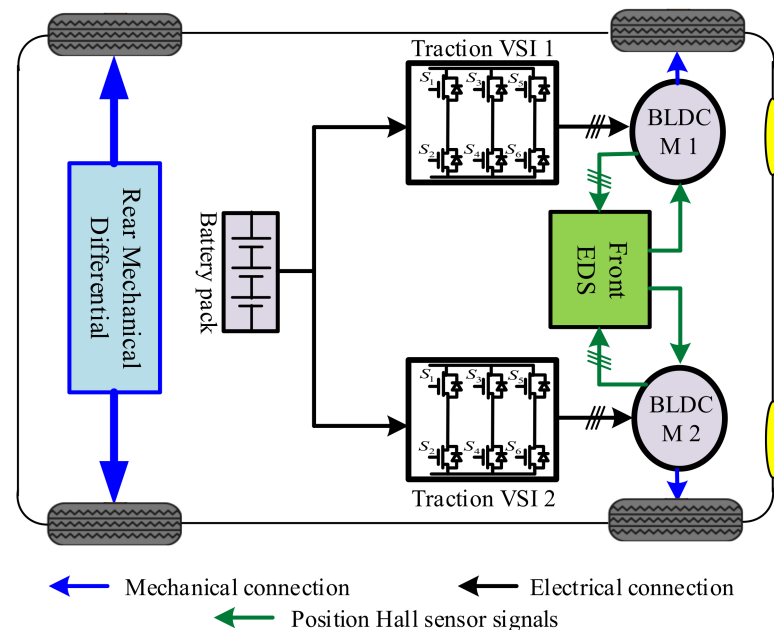

Figure 4. Powertrain system of the EV under study.

The mechanical structure of the EV contains the vehicle body and the wheels' mechanical components. The dynamic of the EV's body movement, during the road surface profile, is defined as

$$M\frac{dv}{dt} = F_m - R(v), \tag{5}$$

where M is the total mass of the vehicle and wheels, v is the vehicle's linear velocity, and F_m denotes the traction force as

$$F_m = \mu(v_s)Mg, \tag{6}$$

where μ is the adhesion factor defined by the nonlinear relation of slip velocity (v_s) [9]. The slip velocity is the difference between wheel and vehicle speed as

$$v_s = r_w\omega_r - v, \tag{7}$$

where r_w is the wheel's radius.

The term $R(v)$ in (5) defines the overall resistance related to the road condition based on the gravitational coefficient g as [9]

$$R(v) = \left(0.000745\,v^2 + 0.0359\,v + 1.867\right)Mg \times 10^{-3}. \tag{8}$$

By considering the above clarifications, the dynamics of an EV mostly depend on the propulsion force deviating from the traction motor's shaft torque as

$$T_{em} = J\frac{d\omega_r}{dt} + B_m\omega_r + F_mr_w, \tag{9}$$

where ω_r and T_{em} are the mechanical angular speed and electromagnetic torque of the traction motors, J is the total inertia of the motor and tires, and B_m is the damping coefficient along with the dynamic model of the propulsion system.

Considering the 2WD EV of Figure 4 equipped with the propulsion system of two BLDC motors on the front wheels, the motion equation of the vehicle is obtained as

$$\frac{dv}{dt} = \left(\mu(v_s) - 7.45 \times 10^{-7}v^2 - 3.59 \times 10^{-5}v - 1.867 \times 10^{-3}\right) \cdot g + \frac{1}{r_w}(u_1 + u_2), \tag{10}$$

where u_1 and u_2 denote the inputs from the traction BLDC motors. On the other hand, considering two BLDC motors with accurate field-oriented control, the operated wheel dynamics can be expressed as [34]

$$\frac{\omega_{r,i}(s)}{u_i(s)} \approx \frac{1}{J_is + B_{m,i}}, \tag{11}$$

where s is the mathematical operator of the differentiator operator, and $i = 1, 2$ denotes the number of traction motors. It should be noted that both motors are empowering the vehicle, and every perturbation on the EV can affect them accordingly. Then, the wheel's dynamics can be considered as

$$J_i\frac{d\omega_{r,i}}{dt} = -B_{m,i} \cdot \omega_{r,i} + T_{L,i} + u_i + \left(\mu(v_s) - 7.45 \times 10^{-7}v^2 - 3.59 \times 10^{-5}v - 1.867 \times 10^{-3}\right) \cdot Mg, \tag{12}$$

where $T_{L,i}$ denotes the external perturbations on the wheel *I*, which comes from the road surface conditions. The Ackermann model connects the EV and wheel speeds to make a unified propulsion system based on two differential equations in (12).

3.3. EDS Model

The electronic differential is generally employed in EVs due to some drawbacks of the conventional mechanical differential such as being heavy assets and the mechanical losses caused by the powertrains. Based on the turning angle of the wheel, the target of an EDS for front wheels is to adjust the angular speed of the wheels. Here, the improved EDS for the studied EV with front 2WD is explained. The Ackermann–Jeantand steering profile is the dynamic model of the outside and inside wheels on a curved road, which is considered to determine the wheel's linear speed. Rudolf Ackermann established the model in the 19th

century. According to Figure 5, the Ackermann model deals with the geometry features of vehicles to properly calculate the steering angle for the wheels [35].
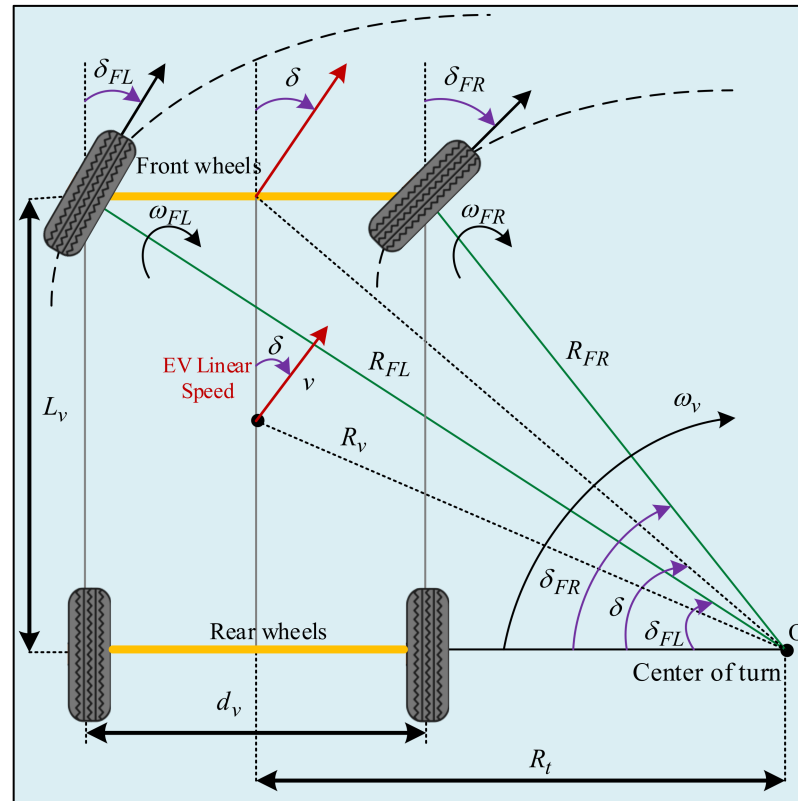

Figure 5. Ackermann steering principle for a vehicle.

The Ackermann EDS principle for an EV with independent speed-controlled wheels is illustrated in Figure 5. The central rotation steering angle of the EV (δ) is determined using a steering sensor. This angle is utilized to set the inner and outer steering angles of the wheels and make decisions regarding the appropriate turning the vehicle in curved paths [10].

Based on Figure 5, the outer (front left) steering angle (δ_{FL}) and the inner (front right) steering angle (δ_{FR}) of the EV's front wheel are calculated as follows:

$$\delta_{FL} = \arctan\left[\frac{L_v \cdot \tan(\delta)}{L_v + ((d_v/2) \cdot \tan(\delta))}\right], \tag{13}$$

$$\delta_{FR} = \arctan\left[\frac{L_v \cdot \tan(\delta)}{L_v - ((d_v/2) \cdot \tan(\delta))}\right], \tag{14}$$

where L_v is the linear distance between the rear and front wheels and d_v is the linear distance between the right and left wheels.

To independently determine the wheels' speeds, the turning radius of the front wheels along with the central radius of the EV (R_v) is given by

$$R_{FL} = \frac{L_v}{\sin(\delta_{FL})}, \tag{15}$$

$$R_{FR} = \frac{L_v}{\sin(\delta_{FR})}, \tag{16}$$

$$R_v = \sqrt{\left(\frac{L_v}{2}\right)^2 + \left(R_t - \frac{d_v}{2}\right)^2}. \tag{17}$$

In (17), R_t is the distance from the vehicle center to the center of turn that is equal to $L_w / \tan \delta$.

As illustrated in Figure 5, when the vehicle is running on a straight road, the angular speed of each front wheel has to be the same regardless of their torque values. It is noted that the chosen speed of the outer wheel must be higher than the inner during such a curved path. Accordingly, based on the Ackermann model, the linear speeds of the front left (FL) wheel v_{FL} and right (FR) wheel v_{FR} are calculated as in (18) and (19).

$$v_{FL} = \omega_v \cdot R_{FL}, \tag{18}$$

$$v_{FR} = \omega_v \cdot R_{FR}, \tag{19}$$

where ω_v denotes the angular speed of the vehicle's differential as v / R_v.

By substituting ω_v in (18) and (19) and the value of the wheel's radius r_w, the desired angular speeds of the front wheels are defined as [10]

$$\omega_{FL} = \frac{R_{FL}}{R_v \cdot r_w} v, \tag{20}$$

$$\omega_{FR} = \frac{R_{FR}}{R_v \cdot r_w} v. \tag{21}$$

Based on the sign and value of δ, it is assumed in this study that the EV turns to the right side if δ is positive, drives on a straight form δ of zero, and turns to the left side for negative δ.

Considering the previous EDS topologies, the stability of the EV during uncertain driving cycles is not fully ensured. Therefore, the main goal of this study is to concentrate on the synchronization of speeds during different road profiles based on the Ackermann principle. To achieve the goal, an improved EDS is presented that deals with combining the rotor positions, which are estimated from the Hall sensor signals of the BLDC motors, to generate a set of switching signals to synchronize/lock the EV's wheels. The proposed EDS drives both BLDC motors with a set of "averaged" signals based on the strategy shown in Figure 5 by synchronizing/locking the rotor angle and speed of the motors if required. The improved EDS differs from a soft-lock approach and conventional designs, which employ a classic PI speed controller for the traction motors through Hall sensor signals [13–20].

From Figure 6, in the first stage, the proposed EDS deals with generating a set of Hall signals ($h_{1,2,3\_mean}$) through appropriate averaging and converting the high-precise rotor positions θ_{r1} and θ_{r2} of the motors, which are predicted from the real Hall signals of the traction drives as $h_{1,2,3\_M1}$ and $h_{1,2,3\_M2}$ based on (2). In the next stage, the EDS applies the common signals $h_{1,2,3\_mean}$ when there is a difference between the rotor positions (i.e., $\Delta\theta_r \neq 0$). It should be clarified that, during the steady-state operation of traction motors of the EV on straight driving cycles, there is a very small difference between the rotor positions, which can mistakenly affect the EDS commanding. To prevent wrong signals being sent to the decoders, a feasible criterion $\Delta\theta_r \neq |\Delta\theta_{th}|$ is selected instead of $\Delta\theta_r \neq 0$ in which $\Delta\theta_{th}$ is a small threshold value. In other words, when $-\Delta\theta_{th} < \Delta\theta_r < \Delta\theta_{th}$, each motor's VSI is operating with its own Hall signals, otherwise the common Hall signals $h_{1,2,3\_mean}$ are transferred to the decoders to fire the VSIs switching devices.

Figure 7 illustrates the procedure of generating the common Hall signals $h_{1,2,3\_mean}$ using the high-resolution rotor positions. Based on Figure 7, the averaged rotor position data $(\theta_{r1} + \theta_{r2})/2$ is converted to degree quantity to shape the appropriate $h_{1,2,3\_mean}$ for commutating the VSI switches during any difference in the rotor positions.
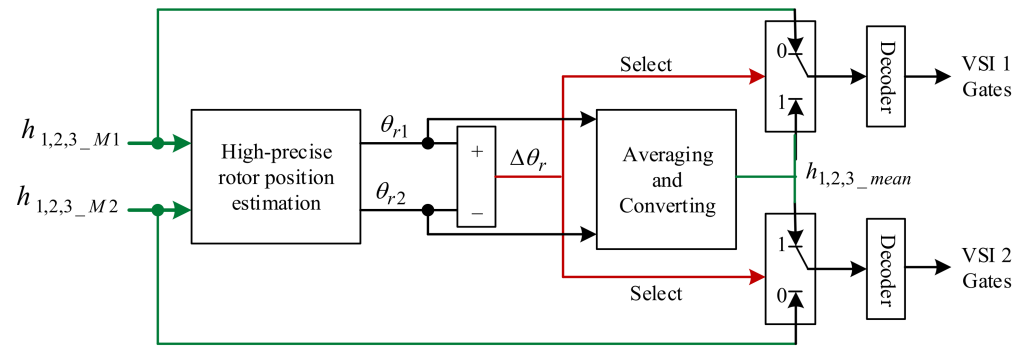
Figure 6. Improved EDS strategy for synchronizing the EV's traction motor drives.
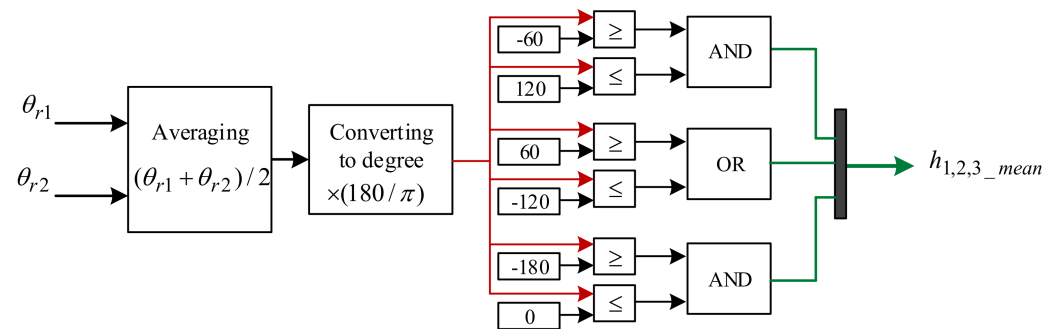

Figure 7. Block diagram of generating the common Hall signals for EDS.

3.4. EV's Drive Control Strategy

The overall control strategy of the EV is illustrated in Figure 8. Based on the aforementioned Ackermann–Jeantand steering model in Section 3.3, the vehicle's linear speed (v) and steering angle (δ) are applied to determine the reference f speeds for each front wheel's BLDC motor. To improve the powertrain performance, closed-loop fuzzy logic algorithm-based speed controllers are employed to properly apply DC voltage to the VSI's DC-link. The estimated angular speed of the motor ω_r is compared to the desired speed ω_{ref}, and the speed error $\Delta\omega_r$ is applied to the speed controller. The speed error for the front-left (FL) $\Delta\omega_{r1}$ and front-right (FR) $\Delta\omega_{r2}$ wheels can be calculated as follows:

$$\Delta\omega_{r1} = \omega_{ref\_FL} - \omega_{r1}, \tag{22}$$

$$\Delta\omega_{r2} = \omega_{ref\_FR} - \omega_{r2}. \tag{23}$$

The outputs of the speed controllers are applied to a variable DC voltage generator to supply the VSIs. The fuzzy logic algorithm-based speed controllers are implemented as shown in Figure 9 by properly determining their membership functions, control roles, and gains [36]. The fuzzy controller includes two inputs: output error $\Delta\omega_r$ and its variation along with membership functions to adjust the rules of the controller. In this study, the values of the fuzzy controllers' gains are determined as G_1 = 0.00008, G_2 = 1.5, and G_3 = 2.
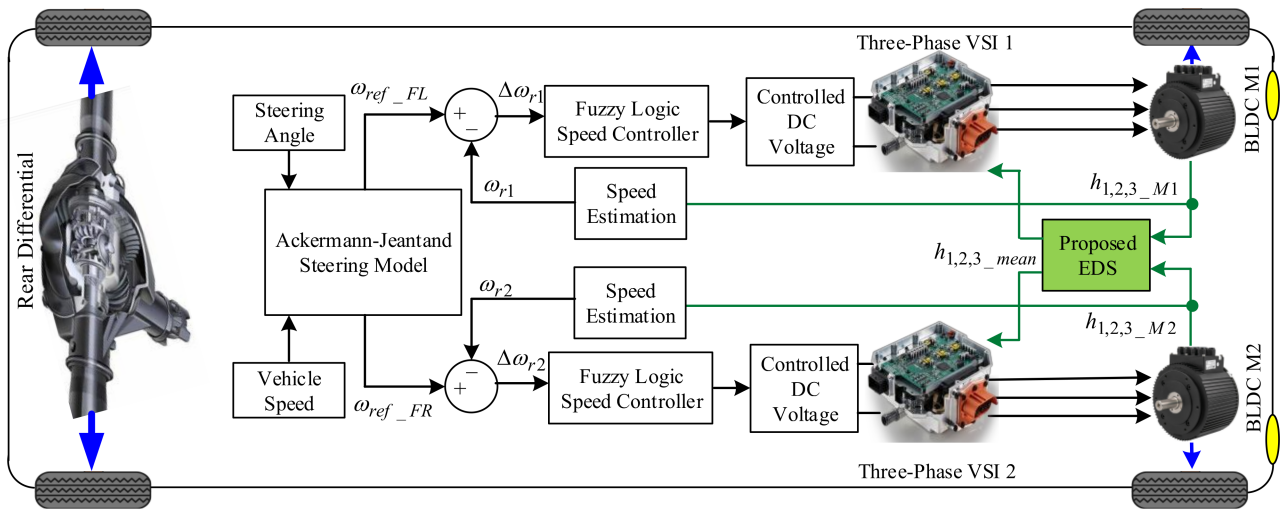
Figure 8. Block diagram of the EV with overall powertrain system.
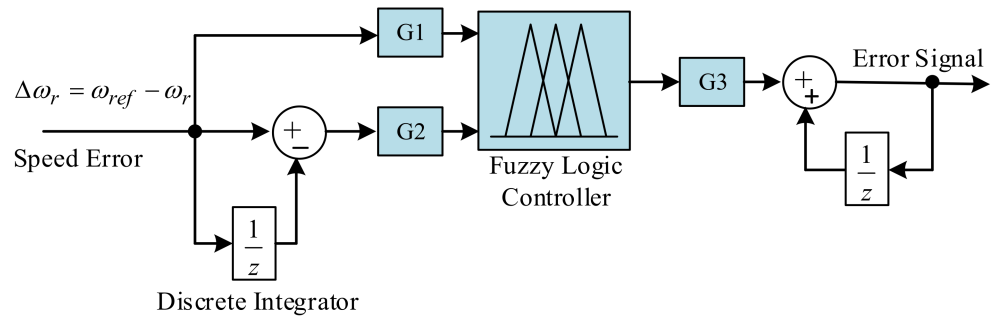

Figure 9. Architecture of the fuzzy controller for the powertrain drive system.

4. Results

To evaluate the effectiveness of the proposed powertrain and the EDS's performance, it is simulated using the MATLAB/Simulink toolbox based on the overall system digital twin model. The employed BLDC motors' parameters and the EV's dynamics are listed in Appendix A. The VSIs are supplied by regulated DC voltage sources with the maximum value of V_{dc} = 48 V, a consequence of a rated speed of 1000 revolutions per min (rpm) for the load torque of 30 N.m. The road surface friction coefficient μ in (6) is determined with the parameters summarized in Table 1, as follows:

$$\mu(v_s) = a_1 \cdot e^{-a_2 \cdot v_s} - a_3 \cdot e^{-a_4 \cdot v_s}. \tag{24}$$

Table 1. Typical friction coefficient values for the case study.

Coefficient \ Parameter	a_1	a_2	a_3	a_4
μ_0 (dry)	1	0.55	1	1.2
μ_1 (wet 1)	0.2	0.55	0.2	1.2
μ_2 (wet 2)	0.1	0.05	0.1	0.5

In this study, various cases with different steering angles and driving cycles are implemented. To assess the EV's stability on wet road surfaces, the EV is subjected to a constant speed on a straight path under a zero steering angle, but with uncertain loads on wheels. Then, the EV is operated on a bumpy road to the left and right corners under a certain load on the wheels. Finally, the EV reverses its direction on the different driving patterns. The common angular speed of the BLDC traction motors is set to a constant value

of 1000 rpm; however, the desired speeds of the motors can be changed because of driving styles and road conditions.

4.1. Case Study 1: Driving with Variable Loads on Wheels

Here, the performance of the proposed powertrain for the EV is analyzed by testing the traction motors with variable torque loads. To validate the EV's performance during unknown road surface conditions, the vehicle is subjected to variable load values based on Table 2 from 27 N.m to 33 N.m at a constant angular speed of 1000 rpm, as depicted in Figure 10. In Table 2, the difference between traction motors' loads is denoted by $\Delta T_L = T_{L2} - T_{L1}$, which can vary from positive to negative values according to the load torques on the motors. From Figure 10a, the BLDC traction motor 1 is started to run at 30 N.m, and then a step change is applied to raise it to 32 N.m at 0.8 s and finally settled at 27 N.m and 1.1 s. However, the BLDC traction motor 2 is started with the same load as motor 1, and then a step to 33 N.m at 0.4 s and settled at 29 N.m at 0.6 s. The output torques of the traction motors are shown in Figure 10b, illustrating the proper track of the loads. Small spikes are seen in the instant speed of the wheels as Figure 10c during load changes on the wheels. Based on the negligible variation between the rotors' angles of the motors (approximately ±0.4 degrees at most based on Table 2), the proposed EDS achieves an appropriate performance level, as illustrated in Figure 10d.
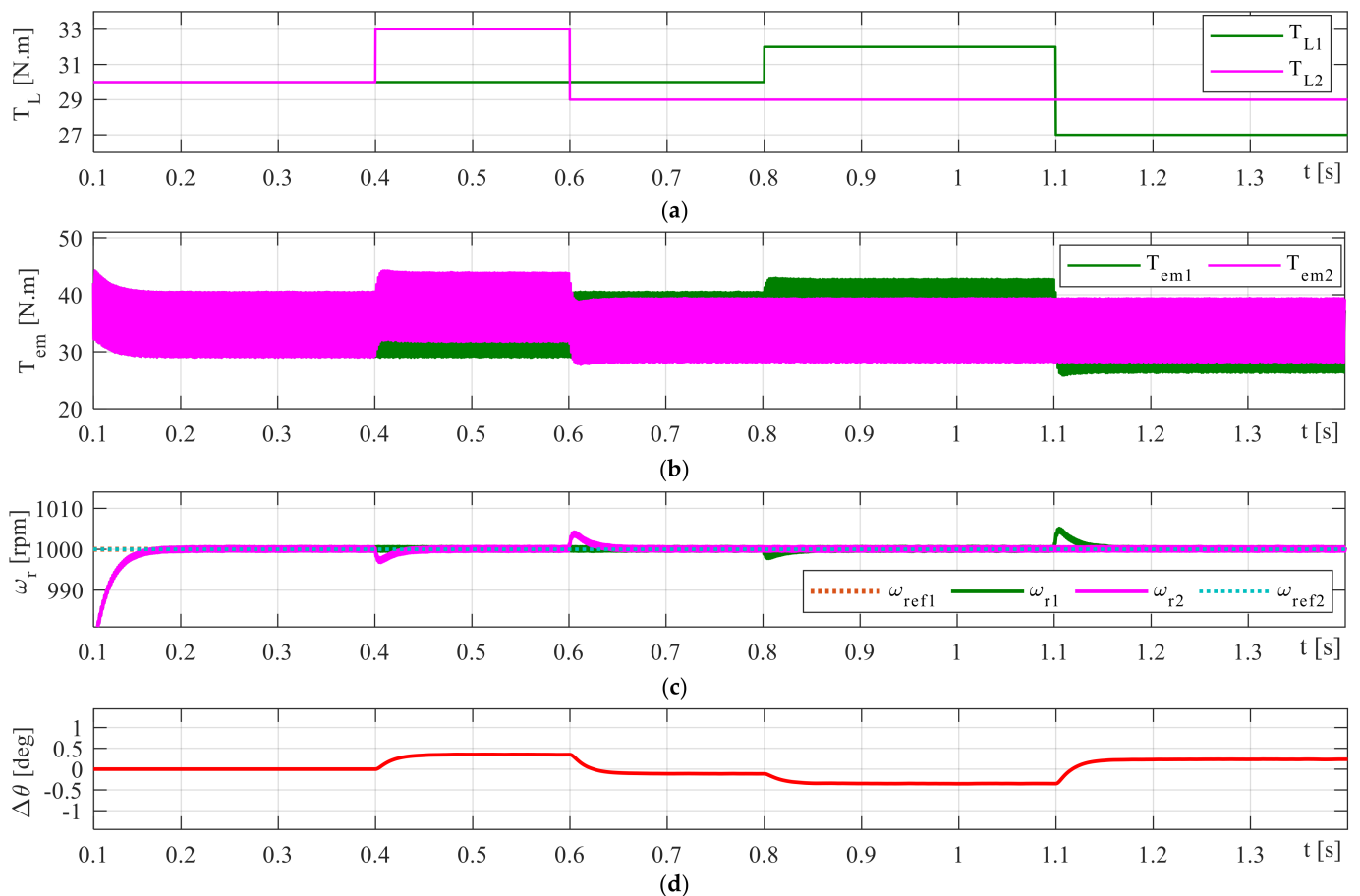

Figure 10. EV's powertrain performance in variable load driving cycles for (**a**) load torque, (**b**) electromagnetic torque, (**c**) speed, and (**d**) rotor position difference.

Table 2. Driving cycle profile for case study 1.

t (s)	0–0.4	0.4–0.6	0.6–0.8	0.8–1.1	1.1–1.4
T_{L1} (N.m)	30	30	30	32	27
T_{L2} (N.m)	30	33	29	29	29
ΔT_L (N.m)	0	3	−1	−3	2
$\Delta\theta$ (deg)	0	0.4	−0.13	−0.4	0.25

4.2. Case Study 2: Driving on Curved Road

In this case study, the accuracy of the proposed powertrain is tested by driving the vehicle in curved paths to the left and right sides with a constant load torque of 30 N.m. To simulate the case, variable positive and negative steering angles are set to drive the motors, first on a straight road, and then the wheel's angle is set to 30 degrees at 0.4 s, 20 degrees at 0.6 s, −20 degrees at 0.8 s, −10 degrees at 1 s, and then settles at a zero steering angle, as illustrated in Figure 11a. From the speed responses in Figure 11b, during changes in the steering angle δ, the desired speeds of the motors are calculated based on the aforementioned Ackermann steering approach and then applied to the powertrain control system to properly turn the vehicle into the corners. The velocity of the traction motors changes during the curved driving cycles to maintain the EV's stability by adjusting the vehicle's common speed (the blue-colored curve in Figure 11b) at a constant speed of 1000 rpm. However, a significant difference is observed in the rotors' angles because of the huge variations in δ, especially from positive to negative.
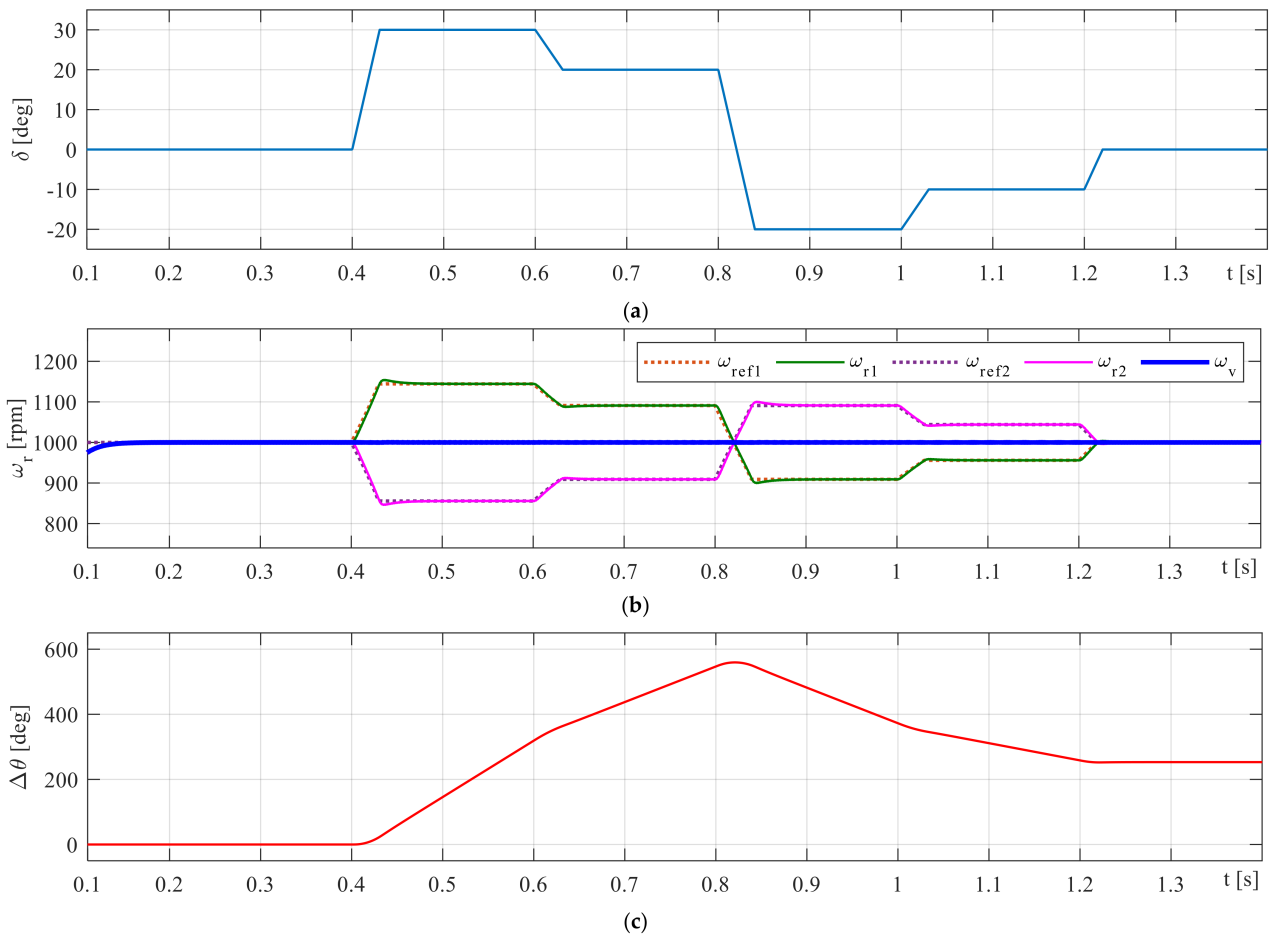

Figure 11. EV's powertrain performance in bumpy driving cycles for (**a**) steering angle, (**b**) speed, and (**c**) rotor position difference.

4.3. Case Study 3: Driving on Uncertain Road Surfaces

To evaluate the overall performance of the EV, it is subjected to uncertain driving cycles with variable surface conditions and steering angles based on Table 3, as depicted in Figure 12. Considering Figure 12a, to start, the steering angle is set to zero, and then is set to 15 degrees at 0.5 s and −15 degrees at 0.9 s. The load torque values are selected as in the first case study (Figure 9a) with a constant speed. Considering the speed and torque responses of the EV's powertrain, the proposed EDS is achieved with decent accuracy by employing a robust high-performance control strategy. It should be noted that the $\Delta\theta$ ranges in Table 3 are approximated by the simulation's numerical results.

Table 3. Driving cycle profile for case study 3.

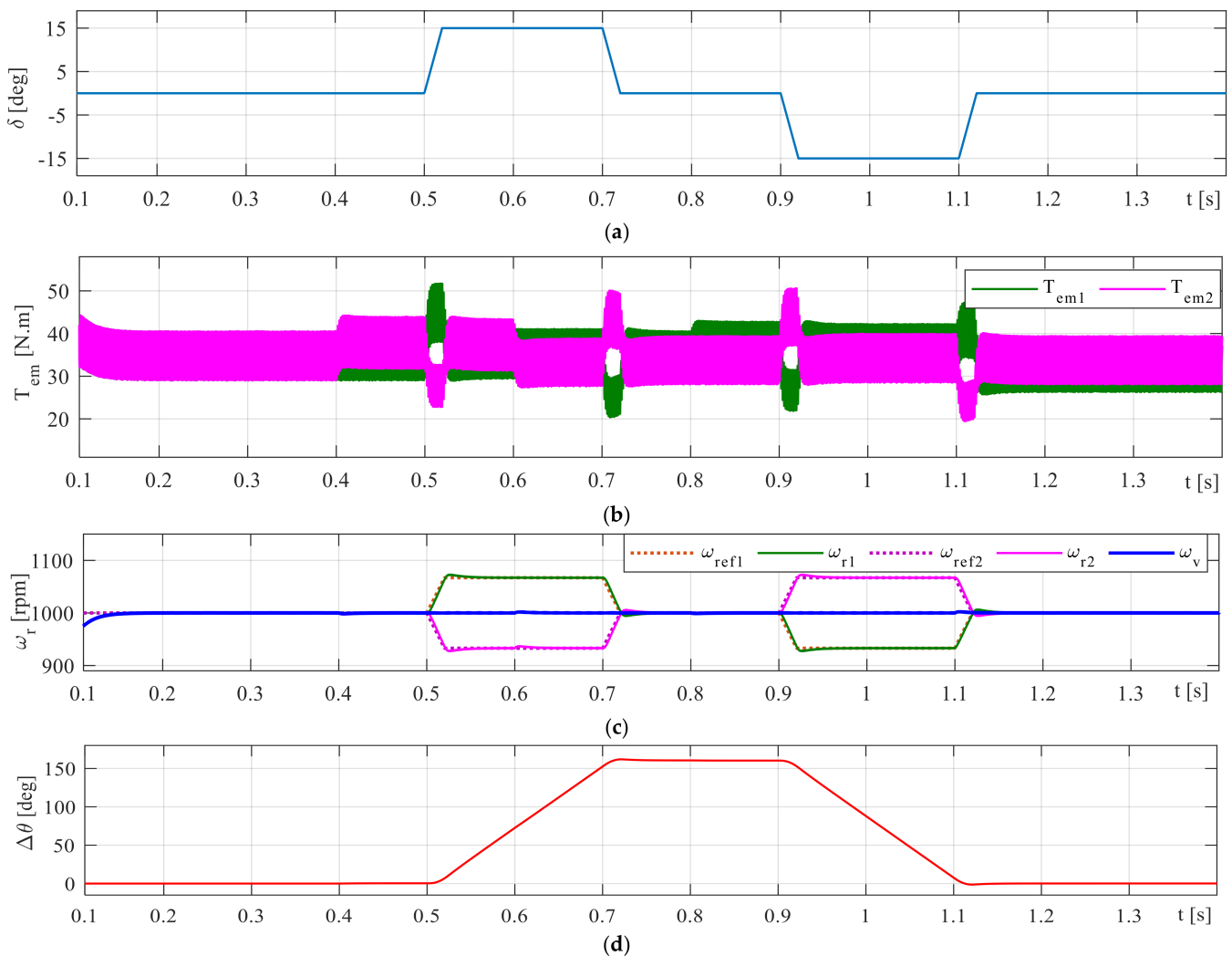| t (s)	0–0.4	0.4–0.6	0.6–0.8	0.8–1.1	1.1–1.4
T_{L1} (N.m)	30	30	30	32	27
T_{L2} (N.m)	30	33	29	29	29
ΔT_L (N.m)	0	3	−1	−3	2
δ (deg)	0	15	0	−15	0
$\Delta\theta$ (deg)	0 << 0.4	0.4 << 160	160	160 << 0.25	0.25

Figure 12. EV's powertrain performance in different road conditions for (**a**) steering angle, (**b**) electromagnetic torque, (**c**) speed, and (**d**) rotor position difference.

4.4. Comparative Studies

To compare the proposed EDS performance with conventional electronic differential systems [13–17] comparative studies are performed on the EV with identical operating conditions. The vehicle is subjected to bumpy driving cycles with constant speed and variable steering angles based on the values listed in Table 4. From Figure 13b, to start, the steering angle is set to zero, and then is set to 25 degrees at 0.7 s and −35 degrees at 0.9 s. From Figure 13c, during the different road surface conditions with zero steering angle (0.3 s to 0.7 s), the operation of the proposed and the conventional EDS is almost identical. On the curved driving cycles from 0.7 s to 1.3 s, the proposed EDS properly follows the references' speeds; however, the conventional EDS is unable to fully track the speed variations and cannot guarantee the desired stability. According to Figure 13d, the EV traction motors' angles are varied in an appropriate way based on the proposed synchronizing/locking strategy to improve vehicle safety in uncertain road conditions, unlike the conventional EDS with low stability. A numerical assessment of the EV with the proposed and conventional EDSs is illustrated in Table 4.
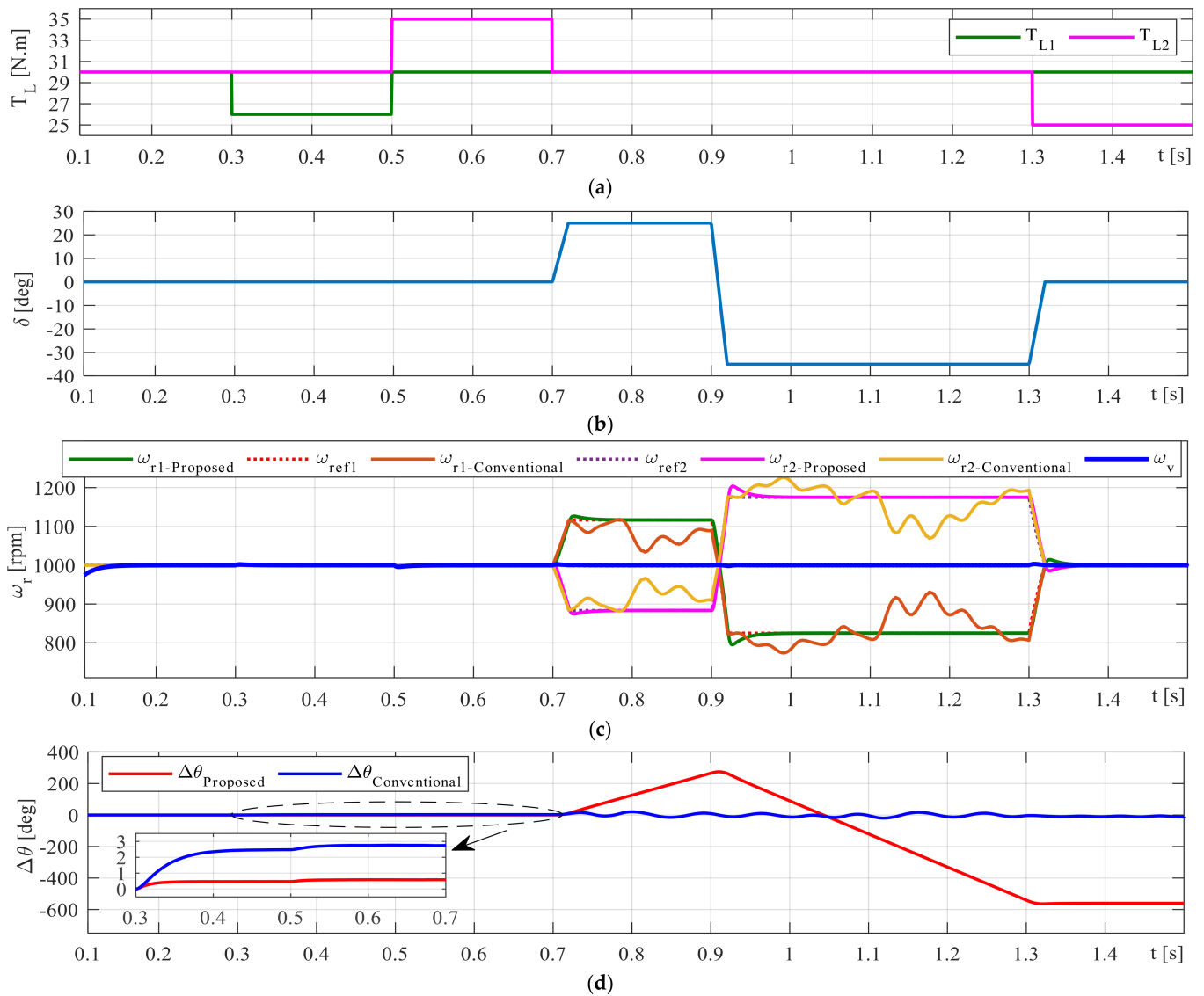

Figure 13. Comparative results in an uncertain driving cycle for (**a**) load torque, (**b**) steering angle, (**c**) peed, (**d**) rotor position differences in proposed and conventional EDS performance.

Table 4. Driving cycle profile for the comparative studies.

t (s)	0–0.3	0.3–0.5	0.5–0.7	0.7–0.9	0.9–1.3	1.3–1.5
T_{L1} (N.m)	30	26	30	30	30	30
T_{L2} (N.m)	30	30	35	30	30	25
ΔT_L (N.m)	0	4	5	0	0	−5
δ (deg)	0	0	0	25	−35	0
$\Delta\theta_{Proposed}$ (deg)	0	0.45	0.55	$0.5 << 255$	$-580 << 255$	−580
$\Delta\theta_{Conventional}$ (deg)	0	2.5	2.9	$-20 << 20$	$-12 << 18$	$-12 << -3$

5. Discussion

The effective separate speed and torque control of 2WD EVs by employing BLDC motor drives are studied with the implementations of various operation scenarios. The improved EDS operates by converting the rotors' angles obtained from the Hall signals of the BLDC motors and transferring the single common signals to enable the inverters. The presented EDS increases the effectiveness of the EV under uneven driving cycles compared to the recent systems. It is depicted that the dynamic variables of each motor follow their desired values due to utilizing the robust speed controllers. The Ackermann–Jeantand model is applied to appropriately calculate the reference values of each key variable. Consequently, the EV can be driven on uneven and bumpy paths stably with less sliding away. The proposed technology, known as IoUEV, which is a modified version of IoTs specified for unmanned electric vehicles, offers various benefits when it comes to undemanding electric vehicles. Specifically, these advantages can be explained in greater detail as follows.

Undemanding electric vehicles that are equipped with the proposed IoUEV technology can be remotely monitored and maintained. This is possible because the IoT sensors installed in the vehicles gather real-time data about important metrics such as the vehicle's performance and battery life. With this data, the vehicle's manufacturer or service provider can identify potential issues and perform proactive maintenance. IoUEV sensors installed in unmanned electric vehicles or IoUEVs can facilitate predictive maintenance by providing real-time data that can be analyzed by manufacturers. This analysis enables manufacturers to detect and address potential issues before they escalate into more serious problems. By scheduling maintenance appointments based on this analysis, manufacturers can help reduce vehicle downtime and ensure that the vehicle operates efficiently at all times. IoUEV-equipped electric vehicles have the potential to be more efficient, resulting in decreased energy consumption and increased battery lifespan. By analyzing sensor data, manufacturers can pinpoint where energy is being inefficiently used and make modifications to improve efficiency. This can result in increased driving range and fewer charging requirements.

By utilizing IoUEVs and the suggested digital twin, the safety of unmanned electric vehicles can be heightened through the provision of up-to-date information regarding weather conditions, road hazards, and other potential risks. This information can be utilized to warn drivers of potential dangers and take preventative measures. Additionally, IoT sensors can recognize when a driver is tired or inattentive, and provide alerts to minimize accidents. The application of IoUEV technology can enrich the user experience of unmanned electric vehicles. For instance, real-time traffic updates and recommended alternate routes can be made available through IoT sensors, as well as assistance in locating open parking spaces. This can improve convenience and driving pleasure for the operator. In general, the proposed IoUEV technology offers substantial benefits for unmanned electric vehicles, especially in the presence of the Metaverse via the suggested digital twin. The inclusion of remote monitoring and maintenance, predictive maintenance, efficiency improvement, safety enhancement, and superior user experience can result in more dependable, efficient, and user-friendly undemanding electric vehicles.

6. Conclusions

This article presented a new approach called "Internet of Unmanned Electric Vehicles" (IoUEVs) that sought to enhance the digitalization of public transportation systems by leveraging the potential of two emerging technologies: the Internet of Things (IoT) and the Metaverse. The research focused on the digital twin section, where a digital twin of an electronic differential system (EDS) was introduced. The EDS had undergone improvements in terms of stability, and it featured robust fuzzy logic algorithm-based speed controllers that allowed for the independent control of electric vehicle (EV) wheels driven by high-performance brushless DC (BLDC) electric motors. The study combined and converted the rotor position information of the motors using low-precision Hall-effect sensors on their shafts to form a set of common switching signals that empowered the electric vehicle traction drive system's EDS. The proposed digital twin EDS relied on an accurate Hall sensor signals-based synchronizing/locking strategy, complemented by a dynamic steering model that ensured the stability of the EV in severe road conditions with different surface profiles. Unlike recent EDSs, the proposed digital twinning approach featured a simple and practical topology that did not require auxiliary infrastructures, reducing mechanical losses and stresses, and it could be adapted to IoUEVs more effectively.

Appendix A

BLDC motor parameters: 4.5 kW, 12 poles, $R = 0.027\ \Omega$, $L = 0.025$ mH, $\lambda_M = 10.9$ mV.s, rotor inertia $J = 0.005$ kg.m^2.

Vehicle mechanical parameters: Mass of the EV, $M_v = 190$ kg, mass of the wheel, $M_w = 10$ kg, total load inertia $J_L = 0.02$ kg.m^2, damping coefficient, $B_m = 0.05$ N.s, radius of the wheel, $r = 0.05$ m, gravitational constant, $g = 9.81$ m/s^2.

References

1. Husain, I.; Ozpineci, B.; Islam, S.; Gurpinar, E.; Su, G.-J.; Yu, W.; Chowdhury, S.; Xue, L.; Rahman, D.; Sahu, R. Electric Drive Technology Trends, Challenges, and Opportunities for Future Electric Vehicles. *Proc. IEEE* **2021**, *109*, 1039–1059. [CrossRef]
2. Sousa, J.D.C.; Sousa, T.J.C.; Monteiro, V.; Afonso, J.L. Traction System for Electric Vehicles Based on Synchronous Reluctance Permanent Magnet Machine. *Electronics* **2023**, *12*, 539. [CrossRef]
3. Eckert, J.J.; Silva, L.C.A.; Costa, E.S.; Santiciolli, F.M.; Dedini, F.G.; Corrêa, F.C. Electric vehicle drivetrain optimization. *IET Electr. Syst. Transp.* **2017**, *7*, 32–40. [CrossRef]
4. Liu, J.; Wang, Z.; Zhang, L. Integrated Vehicle-Following Control for Four-Wheel-Independent-Drive Electric Vehicles Against Non-Ideal V2X Communication. *IEEE Trans. Veh. Technol.* **2022**, *71*, 3648–3659. [CrossRef]
5. Ebadpour, M.; Sharifian, M.B.B. Cascade H-bridge multilevel inverter with low output harmonics for electric/hybrid electric vehicle applications. *Int. Rev. Electr. Eng. IREE* **2012**, *7*, 3248–3256.
6. Tan, S.; Wang, Y.; Cheng, W.; Luo, T.; Zhang, N.; Li, S.; Pan, B.; Cui, X. Cascade Direct Yaw Moment Control for an Independent Eight In-Wheel Motor-Driven Autonomous Vehicle. *Electronics* **2022**, *11*, 2930. [CrossRef]
7. Moazen, M.; Sharifian, M.B.B.; Sabahi, M. Electric Differential for an Electric Vehicle with 4WD/2WS Ability. In Proceedings of the 24th Iranian Conference on Electrical Engineering (ICEE), Shiraz, Iran, 10–12 May 2016; pp. 751–756. [CrossRef]
8. Guo, N.; Zhang, X.; Zou, Y.; Lenzo, B.; Du, G.; Zhang, T. A Supervisory Control Strategy of Distributed Drive Electric Vehicles for Coordinating Handling, Lateral Stability, and Energy Efficiency. *IEEE Trans. Transp. Electrif.* **2021**, *7*, 2488–2504. [CrossRef]

9.   Gougani, M.; Chapariha, M.; Jatskevich, J. Locking Electric Differential for Brushless DC Machine-Based Electric Vehicle with Independent Wheel Drives. In Proceedings of the 2011 IEEE Vehicle Power and Propulsion Conference, Chicago, IL, USA, 6–9 September 2011; pp. 1–6. [CrossRef]

10.   Linus, R.M.; Londhe, S.P.; Shinde, A.N. Implementation of Ackermann's Geometric Electronic Differential Model in PMSM Based Electric Vehicle. In Proceedings of the IEEE 6th Conference on Information and Communication Technology (CICT), Gwalior, India, 18–20 November 2022; pp. 1–5. [CrossRef]

11.   Ebadpour, M.; Sharifian, M.B.B.; Feyzi, M.R. A cost-effective position sensorless control for four-switch three-phase brushless DC motor drives using single current sensor. *Int. Rev. Autom. Control.* **2011**, *4*, 386–393.

12.   Ebadpour, M.; Amiri, N.; Jatskevich, J. Fast Fault-Tolerant Control for Improved Dynamic Performance of Hall-Sensor-Controlled Brushless DC Motor Drives. *IEEE Trans. Power Electron.* **2021**, *36*, 14051–14061. [CrossRef]

13.   Khan-Ngern, W.; Keyoonwong, W.; Chatsiriwech, N.; Sangnopparat, P.; Mattayaboon, P.; Worawalai, P. High Performance BLDC Motor Control for Electric Vehicle. In Proceedings of the International Conference on Engineering, Applied Sciences, and Technology (ICEAST), Phuket, Thailand, 4–7 July 2018; pp. 1–4. [CrossRef]

14.   Kahveci, H.; Okumus, H.I.; Ekici, M. An Electronic Differential System Using Fuzzy Logic Speed Controlled In-Wheel Brushless DC Motors. In Proceedings of the 4th International Conference on Power Engineering, Energy and Electrical Drives, Istanbul, Turkey, 13–17 May 2013; pp. 881–885. [CrossRef]

15.   Khan-Ngern, W.; Keyoonwong, W. Embedded Electronic Differential System on Two Brushless DC Motor Drives for Electric Vehicle Steering Control. In Proceedings of the International Conference on Embedded Systems and Intelligent Technology & International Conference on Information and Communication Technology for Embedded Systems (ICESIT-ICICTES), Khon Kaen, Thailand, 7–9 May 2018; pp. 1–4. [CrossRef]

16.   Al-Fiky, H.T.; Asfoor, M.S.; Yacoub, M.I.; Sharaf, A.M. Electronic Differential Optimization for Electric Vehicle Full Model for In-Wheel Permanent Magnet Brushless DC Motors. In Proceedings of the 7th International Conference on Control, Mechatronics and Automation (ICCMA), Delft, The Netherlands, 6–8 November 2019; pp. 15–20. [CrossRef]

17.   Chhlonh, C.; Riawan, D.C.; Suryoatmojo, H. Independent Speed Steering Control of Rear In-Wheel BLDC Motor in EV Based on Fuzzy Logic Controller in GUI. In Proceedings of the 5th International Conference on Science and Technology (ICST), Yogyakarta, Indonesia, 30–31 July 2019; pp. 1–6. [CrossRef]

18.   Piromalis, D.; Kantaros, A. Digital Twins in the Automotive Industry: The Road Toward Physical-Digital Convergence. *Appl. Syst. Innov.* **2022**, *5*, 65. [CrossRef]

19.   Bhatti, G.; Mohan, H.; Singh, R. Towards the future of smart electric vehicles: Digital twin technology. *Renew. Sustain. Energy Rev.* **2021**, *141*, 110801. [CrossRef]

20.   ElKashlan, M.; Elsayed, M.S.; Jurcut, A.D.; Azer, M. A Machine Learning-Based Intrusion Detection System for IoT Electric Vehicle Charging Stations (EVCSs). *Electronics* **2023**, *12*, 1044. [CrossRef]

21.   Ebadpour, M.; Jamshidi, M.; Talla, J.; Hashemi-Dezaki, H.; Peroutka, Z. Digital Twin Model of Electric Drives Empowered by EKF. *Sensors* **2023**, *23*, 2006. [CrossRef] [PubMed]

22.   Jamil, S.; Rahman, M. A Comprehensive Survey of Digital Twins and Federated Learning for Industrial Internet of Things (IIoT), Internet of Vehicles (IoV) and Internet of Drones (IoD). *Appl. Syst. Innov.* **2022**, *5*, 56. [CrossRef]

23.   Zhang, Z.; Wen, F.; Sun, Z.; Guo, X.; He, T.; Lee, C. Artificial intelligence-enabled sensing technologies in the 5G/internet of things era: From virtual reality/augmented reality to the digital twin. *Adv. Intell. Syst.* **2022**, *4*, 2100228. [CrossRef]

24.   Xiong, M.; Wang, H. Digital twin applications in aviation industry: A review. *Int. J. Adv. Manuf. Technol.* **2022**, *121*, 5677–5692. [CrossRef]

25.   Khalaj, O.; Jamshidi, M.; Hassas, P.; Hosseininezhad, M.; Mašek, B.; Štadler, C.; Svoboda, J. Metaverse and AI Digital Twinning of 42SiCr Steel Alloys. *Mathematics* **2022**, *11*, 4. [CrossRef]

26.   Wang, Z.; Wu, Y.; Niu, Q. Multi-sensor fusion in automated driving: A survey. *IEEE Access* **2019**, *8*, 2847–2868. [CrossRef]

27.   Majumder, U.K.; Blasch, E.P.; Garren, D.A. *Deep Learning for Radar and Communications Automatic Target Recognition*; Artech House: Horwood, MA, USA, 2020.

28.   Gong, J.; Zhang, X.; Lin, K.; Ren, J.; Zhang, Y.; Qiu, W. RF vital sign sensing under free body movement. *Proc. ACM Interact. Mob. Wearable Ubiquitous Technol.* **2021**, *5*, 1–22. [CrossRef]

29.   Shafiei, A.; Jamshidi, M.; Khani, F.; Talla, J.; Peroutka, Z.; Gantassi, R.; Baz, M.; Cheikhrouhou, O.; Hamam, H. A Hybrid Technique Based on a Genetic Algorithm for Fuzzy Multiobjective Problems in 5G, Internet of Things, and Mobile Edge Computing. *Math. Probl. Eng.* **2021**, *2021*, 9194578. [CrossRef]

30.   Roshani, S.; Koziel, S.; Roshani, S.; Jamshidi, M.B.; Parandin, F.; Szczepanski, S. Design of a patch power divider with simple structure and ultra-broadband harmonics suppression. *IEEE Access* **2021**, *9*, 165734–165744. [CrossRef]

31.   Ebadpour, M.; Talla, J.; Jamshidi, M.B.; Peroutka, Z. EKF Digital Twinning of Induction Motor Drives for the Metaverse. In Proceedings of the 20th International Conference on Mechatronics—Mechatronika (ME), Pilsen, Czech Republic, 7–9 December 2022; pp. 1–6. [CrossRef]

32.   Ebadpour, M.; Sharifian, M.B.B.; Babaei, E. Modeling and Control of Dual Parallel BLDC Motor Drive System with Single Inverter. In Proceedings of the 43rd Annual Conference of the IEEE Industrial Electronics Society, Beijing, China, 29 October–1 November 2017; pp. 3740–3743. [CrossRef]

33. Ebadpour, M.; Sharifian, M.B.B.; Babaei, E. Modeling and synchronized control of dual parallel brushless direct current motors with single inverter. *Comput. Electr. Eng.* **2018**, *70*, 229–242. [CrossRef]

34. Perez-Pinal, F.J.; Cervantes, I.; Emadi, A. Stability of an electric differential for traction applications. *IEEE Trans. Vehicular Technol.* **2009**, *58*, 3224–3233. [CrossRef]

35. Choi, M.W.; Park, J.S.; Lee, B.S.; Lee, M.H. The Performance of Independent Wheels Steering Vehicle(4WS) Applied Ackerman Geometry. In Proceedings of the 2008 International Conference on Control, Automation and Systems, Seoul, Republic of Korea, 14–17 October 2008; pp. 197–202. [CrossRef]

36. Ebadpour, M.; Oujghaz, J.T. Improved Electric Differential System for Independent Speed Control of Brushless DC Motors Driven Electric Vehicles. In Proceedings of the 7th International Conference on Control, Instrumentation and Automation (ICCIA), Tabriz, Iran, 23–24 February 2021; pp. 1–5. [CrossRef]